

HoloLens-Based Power Grid Intelligent Inspection System

Di Wu

State Grid Zhejiang Pinghu City Power Supply CO.,
LTD.,
Zhejiang, 314200, China
E-mail: 59876702@qq.com

Jianqiao Pan

State Grid Zhejiang Pinghu City Power Supply CO.,
LTD.,
Zhejiang, 314200, China

Bailang Pan

Pinghu General Electric Installation Company
Zhejiang, 314200, China

Guodong Guo

School of Electrical and Electronic Engineering
North China Electric Power University
Beijing, 102206, China

Abstract—Inspection work in substation is one of the normalization work of operation and maintenance in State Grid Corporation substation, and it is also one of the important means to timely discover the obvious and invisible defects of equipment, which plays a vital role in preventing accidents and ensuring the safe and stable operation of equipment. Therefore, Microsoft's HoloLens is applied to the field of equipment detection and intelligent analysis on power system intelligent inspection in this paper. Since HoloLens can be controlled through the voice, hands of inspectors can be freed. Moreover, real-time data uploading and downloading through HoloLens breaks through the obstacles for experts to effectively obtain real-time data on the spot, and the real-time data display technology of virtual video in intelligent substation as well as expert remote diagnosis functions is realized, which contributes to improving the automation level of intelligent substation inspection.

Keywords—HoloLens; Power Grid Intelligent Inspection; Virtual Video

I. INTRODUCTION

With the rapid development of the domestic economy, the demand for electrical energy is growing, and reliability of power supply plays a vital role in harmony and stability of the whole society, the normal life of the people, and the sustainable development of the economy. Substation is an indispensable part in the smart grid. However, traditional substation inspection and maintenance system has the disadvantages such as low efficiency, low accuracy, large human factors, high management cost, incomplete data storage, etc. Therefore, it is necessary to study a set of intelligent substation inspection system to assist the substation operation management department to perform the substation operation and maintenance work, and intelligent substation construction will be one of the main tasks and key projects in China's smart grid. Moreover, SLAM technology can be used for real-time positioning and map construction, which is common in robot positioning and navigation research. However, due to the large differences in hardware of SLAM related equipment, the algorithm is difficult to integrate, and there are not many practical products on the

market[1-3]. HoloLens outstanding performance in this regard owes to the integration of its configuration. Besides it, based on the SLAM technology, substation inspection personnel can understand the situation through wearable device to complete the route planning navigation, job site collaboration, inspection result entry, and achieve security maintenance. Route design is mainly used in this paper to generate the distance matrix of the equipment to be inspected in the research of the system inspection path planning algorithm where more accurate inspection route can be obtained by optimizing the inspection route.

II. PATROL PATH PLANNING BASED ON SLAM TECHNOLOGY

In order to facilitate the path planning and navigation during the inspection, some road signs need to be set in the process. For example, the door and the location of each device are marked to facilitate the use of the map information. After the above processing, the path planning of the inspection task can be performed according to the task book[4].

In addition to the regular inspection, if it is for some equipment inspection, the equipment listed on the new task list should not be missed, and HoloLens used to automatically generate a patrol path, concatenate the scheduled tasks, and automatically indicate the next task. Therefore, patrol personnel only need to follow the prompts to complete the work order task. In order to save the inspection time, it is necessary to make a reasonable planning of the inspection route.

First, the road signs identifying each device in the map are numbered, and the default door number is No. 1. Then, the communication path of each device is determined according to the ground indicated by the map, and the minimum line distance between each of the devices to be inspected is calculated. Finally, distance matrix is used to generate a distance matrix of the device to be inspected.

$$\begin{bmatrix}
 \infty & 1 & 2 & \dots & n \\
 1 & l_{11} & l_{12} & \dots & l_{1n} \\
 2 & l_{11} & l_{11} & \dots & l_{2n} \\
 \dots & \dots & \dots & \dots & \dots \\
 n & l_{n1} & l_{n2} & \dots & l_{nm}
 \end{bmatrix}$$

The element l_{ij} of the distance matrix represents the minimum polyline distance from device i to device j , and the distance l_{ii} from device i to itself is zero. There are $n-1$ devices to be inspected in the list. Since the inspection always starts from the door, the road sign 1 is always in the first element of the planning sequence. Moreover, such a sequence $1, \dots, s_i, \dots, sn-1$ is needed to be determined where s_i is a certain number from 2 to n , and the range of i is $[1, n-1]$. Besides it, the elements in the entire sequence are different from each other so that the determined inspection distance takes a small value which is shown as follows[5].

$$L = l_{1s_1} + l_{1s_2} + \dots + l_{s_{n-2} s_{n-1}} \quad (1)$$

In the case of fewer devices, the traversal method can be used to fully arrange the various possibilities of the number, and the arrangement of L is minimized. While in the case of more equipment, the heuristic search algorithm can also be adopted to get a better solution. Genetic algorithm whose solution steps are shown in Figure 1 is used in this paper.

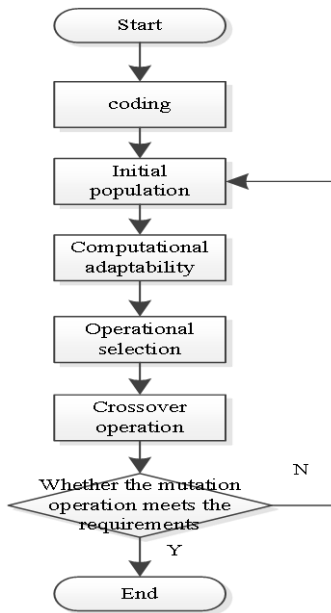


Figure 1. Solution Process of Genetic Algorithm

1) The encoding starts directly with 1 and directly encodes the natural numbers of $1 \sim n$ in a sequence. The data

management service method for substation inspection is as shown in the figure above.

2) The number of individuals in the population is generated by the initial population where M eligible random sequences are randomly generated;

3) The goal is to make L as small as possible with the help of fitness calculation. The smaller L is, the larger fitness J will be. The fitness formula is as follows[6-7].

$$j = \frac{1}{L} \quad (2)$$

4) The calculation is selected to calculate the relative fitness among each individual.

$$F_i = \frac{J_i}{\sum_{k=1}^n J_k} \quad (3)$$

In equation (3) F_i represents the probability that an individual is inherited into the next generation group, and the sum of the total probabilities is 1. In addition, M probability intervals determine M probability intervals. Obviously, the width of each interval is proportional to its relative fitness. What's more, K random numbers from 0 to 1 is generated, and the time the sequence is selected is determined according to the probability interval to which it belongs. Finally, a new group will be generated.

5) The population is randomly paired by crossover operation which keeps the first element unchanged, randomly sets the intersections at other locations, and exchanges the corresponding genes among the paired chromosomes. Since the exchange of chromosome fragments may lead to the repetition or deletion of certain elements in the entire sequence, the chromosome parts outside the exchange area are adjusted accordingly to ensure the integrity and non-repetition of the sequence elements, and the repeating elements are replaced one by one with the missing elements in order. Two identical sub-individuals are generated for the same two parent individuals [8-9].

6) The mutation operation changes the chromosome gene according to a small probability, and the method of changing a sequence in this paper is to exchange some other two elements while keeping the first element unchanged. (3), (4), (5), and (6) are executed repeatedly to a certain number of cycles, which can be stopped until it meets the requirements.

The data management service method for substation inspection is shown in Figure 2.

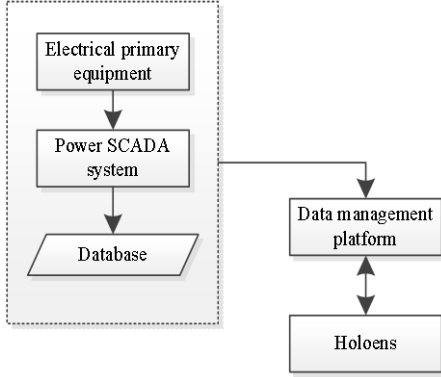


Figure 2. Data Management Service for Substation Inspection

When the inspector transfers SCADA data and historical inspection data, the following steps are required.

1) HoloLens accesses the wifi or 4G private network. The patrol personnel send a request to the data management platform to invoke the Web service through gestures or voices, and queries the real-time status data of the substation equipment.

2) After receiving the request, the data management platform retrieves the basic information of the device to be inspected in the background database, and simultaneously determines whether the data about the device in the existing database is real-time data. If it is real-time, data information will be transmitted to HoloLens[10-11]. Or the acquisition command will be issued through the SCADA system, and the real-time running data of the device will be collected and transmitted back to HoloLens. Then, HoloLens will project the returned data in graphical or tabular form to the current vision of the inspector. Finally, data information will be seamlessly integrated with the reality to provide decision support for the inspectors.

III. MUTATION RECOGNITION ALGORITHM

The offline data of each inspector is 4D vector $\lambda = (\lambda)_{njkh} \in \mathbf{R}_{N_f \cdot N_c \cdot N_s \cdot N_t}$ where n is the frequency serial number, N_f refers to the number of stimulation frequencies, J represents the lead number. What's more, N_c is the number of leads, k indicates the data point, N_s indicates the data length of each trial, h is the trial number, and N_t is the trial number.

Typical correlation analysis of filter bank with template is adopted in the SSVEP recognition algorithm where a plurality of sets from training set data for each subject are averaged to obtain a personal signal template as follows.

$$\bar{\lambda}_{njkh} = \frac{1}{N_t} \sum_{h=1}^{N_t} \lambda_{njkh} \quad (4)$$

Multi-band bandpass filtering is respectively performed on test data λ and template $\bar{\lambda}_n$. The passband of each filter is $(m \times 8) \sim 90$ Hz, m is the sub-band number from 1 to

10, and the number of sub-bands is $N_m=10$. Besides it, filter the Chebyshev-type filter is adopted to obtain the test data and the multiple sets of sub-band components $X_m \bar{\lambda}_{nm} \in \mathbf{R}_{N_c \cdot N_t}$ in the template. CCA analysis is respectively performed on $X_{(m)} \bar{\lambda}_{nm} \in \mathbf{R}_{N_c \cdot N_t}$ as well as standard sine and cosine signals Y_f and $\bar{\lambda}_{nm}$ along with standard sine and cosine signals Y_f to get three sets of spatial filter coefficients $W_{X_m}(X_m, \lambda_{nm})$, $W_{X_m}(X_m, Y_f)$, and $W_{\lambda_{nm}}(\lambda_{nm}, Y_f)$. Correlation coefficient vector \hat{r}_{nm} can be obtained according to the following formula.

$$\hat{r}_{nm} = \begin{bmatrix} r_{n,1m} \\ r_{n,2m} \\ r_{n,3m} \\ r_{n,4m} \\ \dots \end{bmatrix} = \begin{bmatrix} \rho(X_m^T W_{X_m}(X_m, Y_f), Y_f^T W_{Y_m}(X_m, Y_f)) \\ \rho(X_m^T W_{X_m}(X_m, \bar{\lambda}_{nm}), \bar{\lambda}_{nm}^T W_{X_m}(X_m, \lambda_{nm})) \\ \rho(X_m^T W_{X_m}(X_m, Y_f), \bar{\lambda}_{nm}^T W_{X_m}(\bar{\lambda}_{nm}, Y_f)) \\ \rho(X_m^T W_{\lambda_{nm}}(\bar{\lambda}_{nm}, Y_f), \bar{\lambda}_{nm}^T W_{\lambda_{nm}}(\bar{\lambda}_{nm}, Y_f)) \\ \dots \end{bmatrix} \quad (5)$$

In formula (5), $\rho(n, m)$ represents Pearson correlation coefficient between n and m . According to

$$r_{nm} = \sum_{l=1}^4 \text{sign}(r_{n,l_m}) \times (r_{n,l_m})^2 \quad (6)$$

Comprehensive correlation coefficient between the test sample and each frequency template can be obtained.

Finally, according to

$$\rho_n = \sum_{m=1}^{N_m} \alpha(m) \times (r_{nm})^2 \quad (7)$$

$$\eta = \underset{n}{\text{argmax}} \rho_n (n = 1, 2, \dots, N_f) \quad (8)$$

Decision result can be obtained, where $a(m) = m - 1.25 + 0.25$ is the empirical value.

IV. TEST ANALYSIS

A. Performance Evaluation

Recognition accuracy rate and information transmission rate are adopted as the evaluation indicators of BCI system performance in this paper where average value of offline correct rate and ITR are obtained based on the offline experimental data from ten-fold cross-validation in which one signals among 10 sets of offline experimental EEG

signals is selected as the test set, and the other 9 sets are used as the training set, and in the online experiment, each group of online data is identified in real time by using a template based on all offline data to get online recognition accuracy rate and information transmission rate. Moreover, the information transmission rate whose unit is bit/minis an evaluation index widely used in BCI research, which indicates the amount of information transmitted per unit time. The amount of information outputted each time is judged as follows[12-15].

$$\beta = \log_2 N + p \log_2 p + (1-p) \log_2 \left(\frac{1-p}{N} \right) \quad (9)$$

In equation (9), N is the target number, p refers to the recognition accuracy rate, and the information transmission rate is $ITR = \beta(60/T)$ (10) where T is the time required for each instruction to be output.

The information transfer rate is affected by dual factors the time identifying the correct rate and the time required to output a single instruction. In the offline data analysis of this study, the time required to output one instruction is the length identifying the required data plus the stimulation interval. Moreover, offline and online SSVEP recognition accuracy and information transmission rate of each participant on the screen and HoloLens are analyzed in this study, and the difference between the recognition rate and the information transmission rate in offline and online experiments in computer screen-based BCI and HoloLens-based AR-BCI were compared by statistical analysis.

B. Correct Rate

First, the correct rate of 12 subjects in HoloLens, off-screen, and online experiments with different data lengths (0.5-2.0 s, interval 0.1 s) is calculated and compared, which is shown in Figure 3.

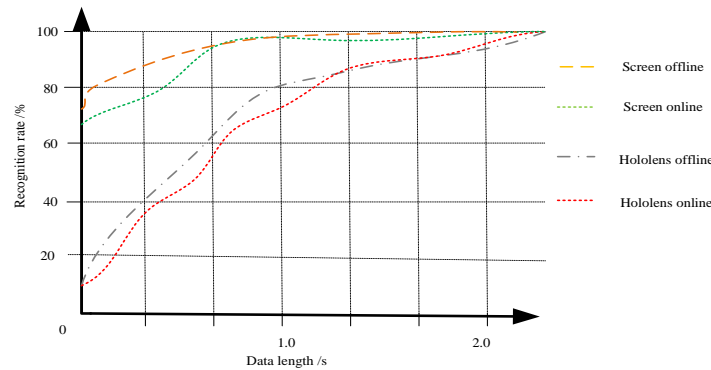


Figure 3. Offline and Online Recognition Accuracy Rate in Screen and HoloLens

Here, the classification accuracy rate when the data length is 0.5, 1.0, 1.5, and 2.0 s is specifically compared, and the mean value is shown in Table 1.

TABLE I. IDENTIFICATION ACCURACY RATE AT DIFFERENT DATA LENGTHS

Experimental condition	Device	data length/s			
		0.5	1.0	1.5	2.0
Offline	Screen	87.8 ± 12.0	98.3 ± 3.0	99.0 ± 2.2	99.0 ± 2.2
	HoloLens	50.9 ± 14.8	87.1 ± 8.2	95.0 ± 3.3	97.5 ± 2.0
Online	Screen	75.8 ± 20.1	94.8 ± 7.3	98.8 ± 2.0	99.0 ± 2.0
	HoloLens	48.6 ± 14.3	88.7 ± 6.0	95.8 ± 2.9	98.6 ± 1.7

It can be seen from Table 1 that the classification accuracy rate increases with the increase of the data length. When the data length reaches 1 s, the average correct rate reaches 87.1% under the four conditions. When the data length reaches 1.5s, the average correct rate under all four conditions is above 95.0%, and when the data length reaches 2s, the average correct rate is above 97.5% under the four conditions. What's more, when the data length is small (less

than 1 s), the correct rate of AR-BCI recognition based on HoloLens is lower, which is significantly lower than the ordinary BCI based on the screen. However, when the data length is large (more than 1.5s), the difference between AR-BCI and ordinary screen BCI is not obvious. Additionally, two-way analysis on variance is performed on offline and online classification accuracy rates, and the effects of visual stimulation equipment (screen, HoloLens)

and data length (0.5, 1.0, 1.5, 2.0 s) on the correct rate are statistically analyzed as well. The results are shown in Table 2.

TABLE II. VARIANCE ANALYSIS RESULTS OF CORRECT RATE

Experimental condition	factor	Degree of freedom	F value	P
Offline	Data length	3, 88	75.75	<0.01
	device	1, 88	74.39	<0.01
	Interaction	3, 88	27.24	<0.01
Online	Data length	1, 88	78.39	<0.01
	device	1, 88	22.86	<0.01
	Interaction	3, 88	10.31	<0.01

Under offline and online conditions, both device factors and data length factors have a significant impact on the recognition accuracy rate, and there is a significant interaction between the stimulus device and the data length, which can be seen from Figure 3 and Table 2, when the data length is large, the device factor has little effect on the correct rate of SSVEP recognition.

In order to deeply explore the difference of the correct rate between the two devices under different data lengths, the paired t-test is performed on the screen and HoloLens correct rate under offline and online conditions with different data lengths (0.5, 1.0, 1.5, 2.0s), and the difference between the correct rate and the HoloLens is compared as well. The results are shown in Table 3.

TABLE III. PAIRING T TEST RESULTS OF CORRECT RATE

Experimental condition	Data length/s	Degree of freedom	t value	P
Offline	0.5	11	-6.35	<0.01
	1.0	11	-5.84	<0.01
	1.5	11	-3.93	<0.01
	2.0	11	-1.8	0.10
Online	0.5	11	-3.92	<0.01
	1.0	11	-2.72	<0.05
	1.5	11	-3.32	<0.01
	2.0	11	-0.46	0.65

It can be seen from Table 3 that when the data length is small, the screen-based BCI correct rate is significantly larger than that of the HoloLens-based AR-BCI whether offline or online, and as the data length increases significantly, there is no significant difference in the recognition rate of SSVEP between the screen and HoloLens when the data length reaches 2s.

V. CONCLUSION

SSVEP-based grid intelligent inspection system which can successfully induce obvious SSVEP in the AR scenarios studied with the help of Microsoft HoloLens AR equipment in this paper where an average of 88.67% (78%~100%) online recognition accuracy can be realized with the help of the data whose length is 1s, and the average online recognition accuracy of 98.6% can be achieved by using data whose length is 2s. Substation field operations require high

quality and skill due to its wide range of equipment, professionalism and security risks. Exploitation on HoloLens-based substation intelligent auxiliary patrol system provides on-site personnel with real-time guidance and auxiliary information highly integrated on-site environment, supports back-end expert team to correct on-site personnel error operation and provides remote assistance in time to ensure the safety, standardization and high efficiency on on-site operation, which is of great significance to improve the level of on-site operation in the substation.

REFERENCES

- [1] Ren Yongqiang, Zhang Qiangqiang. DELMIA based main reducer and differential assembly assembly simulation [J]. Combined machine tools and automated machining technology, 2016 (11): 122-125.

- [2] Li Wei, Chen Jianing, Zhang Linwei. Application Research of Mixed Reality Technology in Nuclear Power Plant Equipment Maintenance [J]. *Computer Simulation*, 2018, 35(5): 340-345.
- [3] Tang Zhuohui, Zhu Peiyi. Virtual reality, augmented reality and mixed reality and its application in the rail transit industry [J]. *Railway Communication Signal Engineering Technology*, 2016, 13 (5): 79-82.
- [4] Shi Lei, Luo Tao, Zhang Li, et al. Preliminary application of HoloLens glasses in liver cancer resection [J]. *Journal of Central South University (Medical Sciences)*, 2018, 43 (5): 500-504.
- [5] Shao Zhaotong, He Bing, Chu Yi. Application Research of Mixed Reality Technology in Construction Engineering [J]. *Civil Engineering Information Technology*, 2017, 9(3): 43-46.
- [6] Chu Yi, Shao Zhaotong, Wu Tao. Discussion on Application of Information Construction Engineering Based on MR+BIM Technology[J]. *Civil Engineering and Information Technology*, 2017, 9(5): 94-97.
- [7] Xie Jiacheng, Yang Zhaojian, Wang Xuewen, et al. Research on virtual assembly and simulation system design and key technology of mining equipment [J]. *Journal of System Simulation*, 2015, 27(4): 794-802.
- [8] Hu Hong, Qi Jiangang, Lin Wanhong, et al. Astronaut virtual assembly training simulation method based on virtual hand interaction [J]. *Computer Application*, 2015(S2):200-203.
- [9] Li Jing, Zhang Lijun, Ren Tianmeng. Research on interactive engine virtual assembly system [J]. *Manufacturing Automation*, 2017, 39(2): 109-113.
- [10] Wen Huaixing, Zhu Xiaojie. Research on virtual assembly technology of headstock based on EON CNC lathe [J]. *Combined machine tools and automated machining technology*, 2015 (11): 107-110.
- [11] Ma Shuai. Research on virtual simulation and augmented reality application technology of mechanical products based on Unity3D [D]. Shijiazhuang: Hebei University of Science and Technology, 2017.
- [12] Nakanishi M, Wang YJ, Chen XG, et al. Enhancing detection of SSVEPs for a high - speed brain speller using task-related component analysis [J]. *IEEE Transactions on Biomedical Engineering*, 2018, 65(1) : 104-112.
- [13] Wang H, Zhang Y, Waytowich NR, et al. Discriminative feature extraction via multivariate linear regression for SSVEP -based BCI [J]. *IEEE Transactions on Neural Systems and Rehabilitation Engineering*, 2016, 24(5) : 532-541.
- [14] Krucoff MO, Rahimpour S, Slutzky MW, et al. Enhancing nervous system recovery through neurobiologics, neural interface training, and neurorehabilitation [J]. *Frontiers in Neuroscience*, 2016, 10: 584.
- [15] Horii S, Nakauchi S, Kitazaki M. AR-SSVEP for brain-machine interface: Estimating user's gaze in head-mounted display with USB camera [C] // *Proceedings of the IEEE Virtual Reality Annual International Symposium*. Paris: IEEE, 2015: 193-194.